Journal of the European Ceramic Society **19** (1999) 2039–2047
© 1999 Elsevier Science Limited
Printed in Great Britain. All rights reserved
PII: S0955-2219(99)00036-9 0955-2219/99/$ - see front matter

Pressureless Sintering of Bioverit® III/Ti Particle Biocomposites

E. Verné,[a]* M. Ferraris[a] and C. Jana[b]

[a]Materials Science and Chemical Engineering Department, Polytechnic of Torino, C.so Duca degli Abruzzi 24, 10129, Torino, Italy
[b]Friedrich-Schiller-Universität Jena, Otto-Schott-Institut, Fraunhoferstraße 6, D-07743 Jena, Germany

(Received 29 July 1998; accepted 10 January 1999)

Abstract

A new bioactive material, based on Bioverit® III glass-ceramic (B3), was synthesised: it is a composite material (named B3T) having a glass-ceramic matrix and titanium particles as toughening phase. The aim was to toughen the Bioverit® III glass-ceramic, already successfully tested by in vivo *experiments. The B3T biocomposite, reinforced by 15 vol% Ti particles, was prepared by pressureless sintering, starting from Bioverit® III base glass powders. The sintering conditions were carefully optimised by using differential scanning calorimetry and hot stage microscopy. On the basis of this study a low temperature viscous flow sintering process was chosen, and high density glass-matrix composites were obtained. A further crystallisation, using the temperature and time conditions for bulk Bioverit® III glass ceramic, was performed to obtain a glass-ceramic matrix/Ti particle composite. A qualitative mechanical characterisation revealed toughening benefits in the Ti additions. An* in vitro *test (fibroblast growth) was performed on the composites in order to demonstrate their biocompatibility. © 1999 Elsevier Science Limited. All rights reserved*

Keywords: titanium particles, sintering, composites, glass ceramics, biomedical applications.

1 Introduction

One of the most investigated materials for bone reconstruction and substitution is bioactive glass and glass-ceramic. These materials are characterised by a high biocompatibility and tight bonding to bone, resulting from the growth of healthy tissue directly onto their surface. Due to their limited fracture toughness, these bioactive materials do not always have the mechanical properties required in prosthetic devices (i.e. load bearing). For that reason composite materials have been developed, with the aim of combining the properties of the bioactive material with the toughness or the tensile strength of a second phase. These composite materials include: stainless steel fibre/bioactive glass, titanium fibre/bioactive glass, ceramic particle/bioactive glass-ceramic composites, and several ceramic/bioactive ceramic composites.[1]

The fabrication methods can vary depending on the amount of the reinforcing phase, its geometry, and the chemical composition and thermomechanical properties of the matrix. The processing parameters have to be optimised to assure a correct and effective stress transfer between the matrix and the reinforcing phase. That means, in many cases, that a continual and strong interface must be obtained. Bioverit® III[2–4] is a bioactive phosphate based glass-ceramic which does not contain silica; it comprises as crystalline phases apatite, aluminium phosphate and complex phosphates. Its composition belongs to the P_2O_5–Al_2O_3–CaO–Na_2O system, and it shows an 'invert glass' structure, formed by mono- and diphosphate units.[2] *In vivo* experiments have shown its high bioactivity.[2]

In this work a Bioverit® III glass-ceramic matrix composite, containing Ti particles as toughening phase, was prepared, in order to improve the low mechanical properties. The preparation process was carefully optimised in respect to density, continuity of the glass-ceramic/metal interface, toughness and bioactivity of the composite.

---

*To whom correspondence should be addressed.

2 Experimental Procedure

The base glass of Bioverit® III (B3) was prepared by melting high purity raw materials. Its chemical composition is (wt%): 51·4 P_2O_5, 16·0 CaO, 9·0 Al_2O_3, 14·6 Na_2O, 1·8 F, 4·5 ZrO_2, 2·7 TiO_2. Density measurements (Archimedean method) were performed on bulk glass specimens. The bulk glass was ball-milled, sieved up to 80–100 μm, and submitted to a thermal scan between 50 and 700°C (heating rate 10 K min^{-1}, under Ar flow) by means of differential scanning calorimetry (Perkin–Elmer DSC7) in order to determine its characteristic temperatures. The same analysis was performed on a bulk glass specimen and on a small cube of pressed glass powder, in order to compare the behaviour of the glass in the three different forms during heating.

In order to prepare the Bioverit® III composite (B3T), a sintering process was optimised by means of differential scanning calorimetry (DSC) and hot stage microscopy. The glass powders were mixed with 15 vol% Ti particles (Plasma Technik 99·99% purity, size = 40–50 μm). The linear shrinkages of the glass and glass plus Ti powders were measured between room temperature and 1000°C on green cubes of $3\times3\times3\,(\mathrm{mm})^3$ size (heating rate 10 K min^{-1} under Ar flow) by means of hot stage microscopy (Leitz Mod. II A). As described in previous works,[5–7] some isothermal treatments (30 min) were performed on glass- and glass plus Ti powders, in the temperature range between the glass transition ($T_g = 493 \pm 2°C$) and the first crystallisation temperature ($T_{x1} = 597 \pm 2°C$), under Ar flow. After isothermal treatment, each sample was submitted to a DSC temperature scan (400–700°C, heating rate 10 K min^{-1}), in order to identify a temperature range in which a 30 min isothermal treatment did not induce any or little crystallisation of the glass. A simulation of the sintering process was also carried out by hot stage microscopy, with isothermal treatment of glass- and glass plus Ti green cubes, in the same temperature range as the calorimetric study, in order to determine the conditions for the highest shrinkage. In this way, a viscous flow sintering temperature range was found.

Unfired compacts of the glass plus Ti powders were prepared by uniaxial cold-pressing using a pressure of 193 MPa, reaching a green density of 67% of the theoretical values. The green samples were then pressureless sintered for 30 min, under Ar flow, at 530, 540, 550 and 560°C. These temperatures were chosen on the basis of the previously described thermal studies. Some samples were sintered at 620, 750 and 790°C, temperatures corresponding to the maximum shrinkage range, but at which a certain degree of crystallisation could occur. As a reference, green samples of pure glass were sintered under the time and temperature conditions which led to the best sintered composites. Density measurements were performed on the sintered samples by different methods. The apparent density was determined by the Archimedean method. In order to evaluate the relative density in respect to the true one, the true density of the sintered samples was determined by liquid picnometry on the powdered composites. The relative density was then calculated as the ratio between the apparent density and the picnometric density as follows:

$$d_{\%} = \left(\mathrm{d_a}/\mathrm{d_p}\right)100$$

where: $\mathrm{d_a}$ = apparent density, $\mathrm{d_p}$ = picnometric density (true density).

The temperature which led to the highest relative density was finally chosen as the preferred sintering temperature.

All sintered samples were characterised by means of XRD (Philips PW1830), SEM (Philips 525 M), EDX (Philips - EDAX 9100); mechanical tests (Young's modulus, induced crack propagation by Vickers indentations) were performed on the samples sintered at the optimised temperature. In order to obtain glass–ceramic matrix composites, the glass-matrix sintered composites were successively ceramised by the thermal treatment normally used to prepare the bulk glass–ceramic, as reported in the literature.[8] The glass–ceramic samples were then characterised by means of SEM, EDX, XRD, Young's modulus measurements, induced crack propagation. The K_{IC} was also determined by an indentation technique, using the following formula.[9,10]

$$K_{IC} = \mathrm{A}(E/H)^{1/2}\left(P/c_0^{3/2}\right)$$

where:

A = constant (= 0·016) not depending on the tested material;
E = Young's modulus of the material;
H = Vickers hardness of the material;
P = indentation load;
c_0 = average value of the cracks length, measured from the centre of each indent.

Biocompatibility tests were performed both on glass- and glass-ceramic matrix B3T composites by cell growth experiments. Animal fibroblast culture tests were performed at the Pathological Anatomy Institute (Veterinary Faculty, University of Torino). The samples, previously cleaned in a 1:1 mixture of diethyl ether and ethanol (70%), rinsed with distilled water and sterilised for 2 h at 150°C, were placed in a Petri capsule for cell culture and incubated in CO_2, at 37°C for 48 h. As a reference a 'cell culture grade' specimen was used. The specimens were then rinsed with a saline solution, fixed with formaline and glutaraldehyde, dried and metallised for SEM investigations.

3 Results and Discussion

3.1 Thermal properties

Figure 1 shows the DSC thermograms performed on a B3 bulk base glass specimen (a), on B3 cold pressed base glass powders (b), on as sieved B3 base glass powders (c), and on as sieved B3 base glass plus 15 vol% Ti powders (d). The onset temperature of the first crystallisation peak is at about 570°C both in the case of the as sieved powders and of the pressed ones (see curves b and c), while in the case of the bulk glass (curve a) crystallisation occurs only above 650°C. This feature is likely to be related to a surface crystallation mechanism. The curve d, relative to the glass plus Ti powders, shows the same crystallisation peak onset temperature of the pure as sieved glass, even if a certain difference in the shape of the peak is evident.

The fact that curves b and c showed the same crystallisation onset temperature allowed to perform the calorimetric study of the sintering process on the as sieved glass powders, and to correlate the results with those obtained by hot stage microscopy of the composite compacts.

The temperature scan performed by hot stage microscopy on glass- and glass plus Ti compacts gave information about the softening range and about the maximum percent linear shrinkage. The linear shrinkages of B3 (base glass) and B3T (glass-matrix composite) powder compacts, during the scan between room temperature and 750–1000°C are reported in Fig. 2. The glass undergoes a fast shrinkage above 490°C. The highest linear shrinkage (18%) is between 540 and 550°C, and the crystallisation of the glass occurs with no volume expansion detectable with this technique. The linear shrinkage was not measurable above 750°C, because of the progressive softening and subsequent melting of the glass powders. Also in the case of the B3T compact the highest shrinkage (16%) occurs between 540 and 550°C, remaining constant up to 800°C. The percentage of linear shrinkage is comparable for both the glass and the composite compacts and occurs in the same temperature range. Only above 800°C, at temperatures close to the glass melting range, does a rapid expansion take place in the presence of Ti. Therefore, the temperatures suitable for the sintering process optimisation have been firstly individuated in the range between T_g and 790°C.

3.2 Sintering process simulation

The formation of crystalline phases during the glass-matrix greens sintering could affect the particles viscous flow, resulting in a low density product.[5] Therefore, as discussed in previous works,[5–7] the sintering conditions must be chosen in order to have the best compromise between

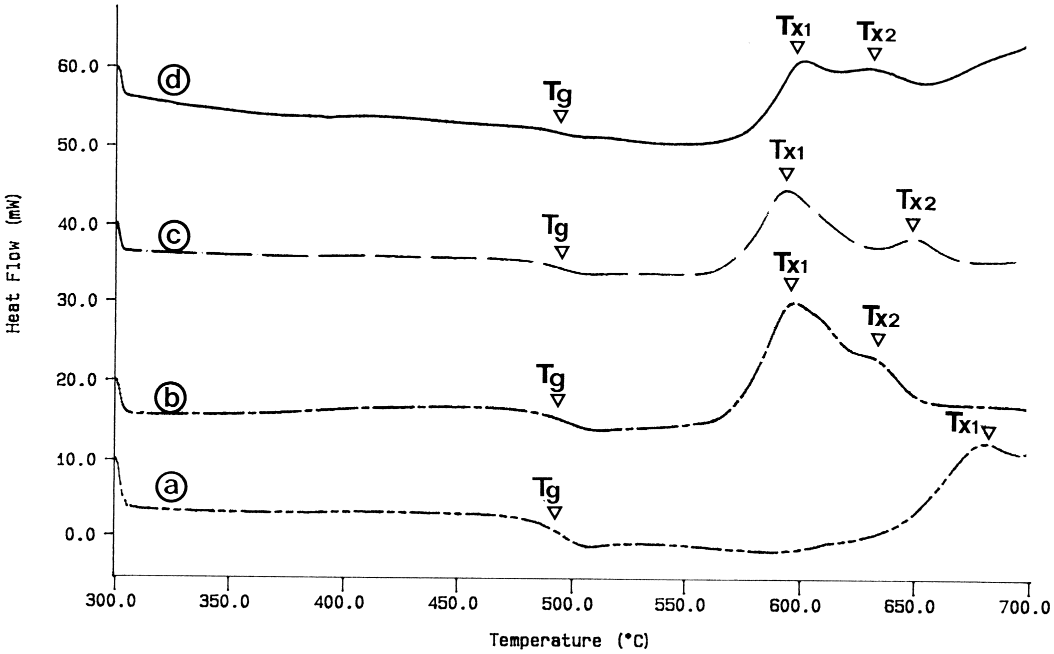

Fig. 1. Thermograms of a B3 bulk base glass specimen (a), B3 base glass pressed powders (b), B3 as sieved base glass powders (c), and as sieved B3 base glass plus 15 vol% Ti powders (d).

low viscosity (i.e. high temperature and low crystallinity. The calorimetric study of the sintering process was performed in the temperature range in which the highest shrinkage occurs. Figure 3 reports the DSC scans, between 300 and 700°C, carried out on B3 base glass powders previously isothermally heated for 30 min at the temperature indicated on each curve. By comparing these thermograms it is evident that above 540°C a 30 min isothermal treatment induced a partial crystallisation of the glass (the crystallisation peak becomes less intense), while up to 530°C the glass could be isothermally treated for 30 min with no alteration in the crystallisation behaviour. Similar results were obtained on the B3 plus Ti powders.

In order to evaluate the linear shrinkage of both glass- and glass plus Ti particles during isothermal heating conditions, some isothermal treatments were performed on small green cubes, by hot stage microscopy, at the same temperatures as those used in the calorimetric study. The highest shrinkage was reached for each sample after 30 min at 550°C, in keeping with the linear shrinkage recorded by hot stage microscopy during the scan between room temperature and 750–1000°C.

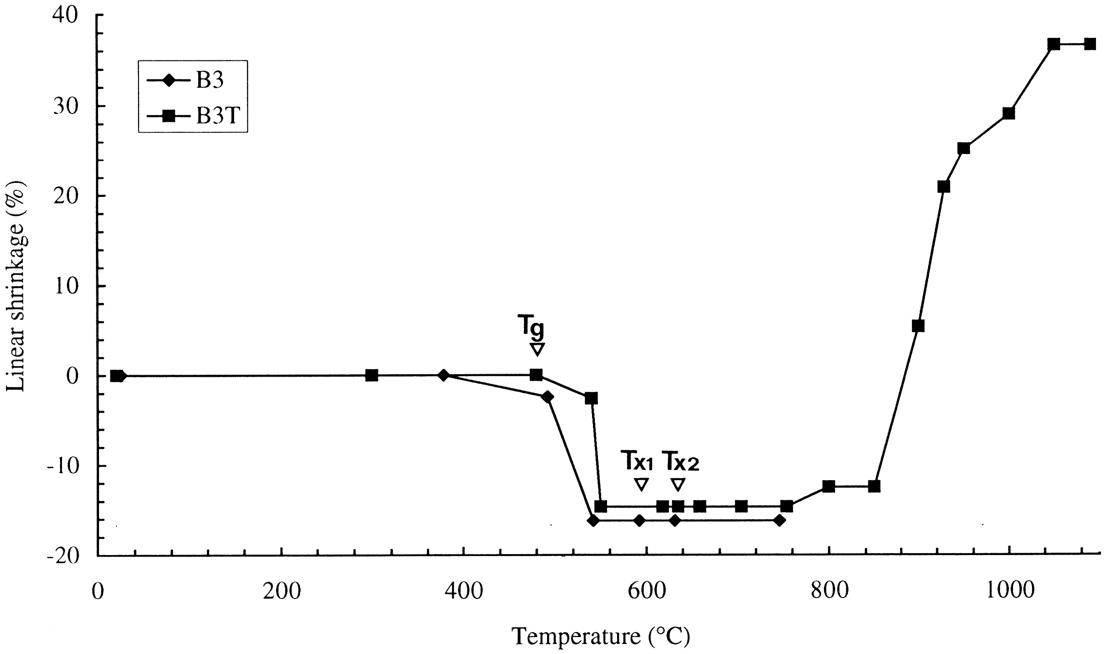

Fig. 2. Linear shrinkages of B3 (base glass) and B3T (glass-matrix composite) greens.

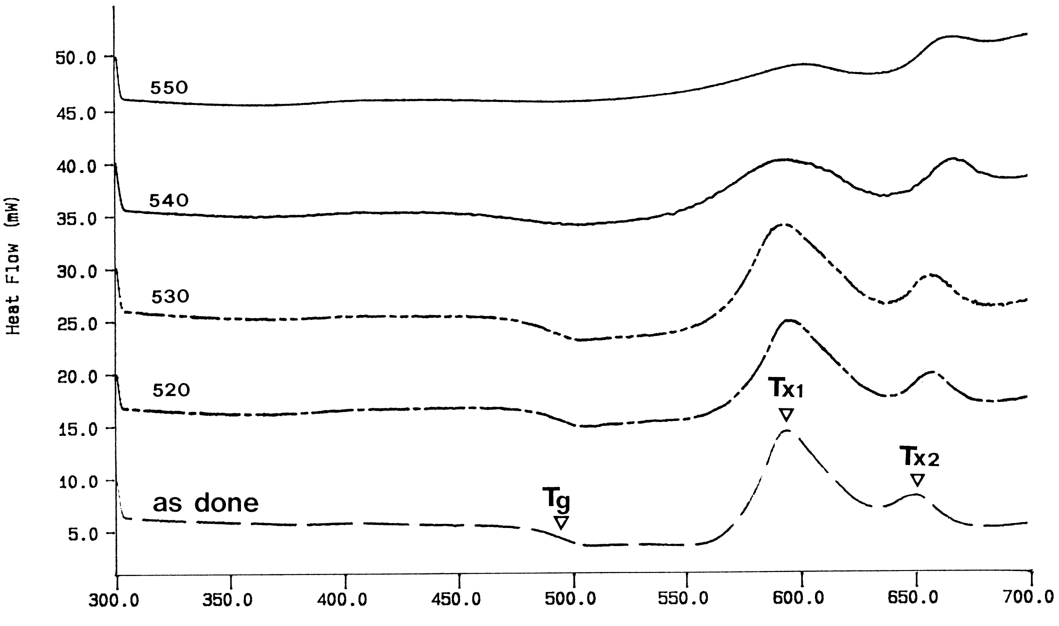

Fig. 3. Thermograms of the B3 base glass powders isothermally treated 30 min at the temperature labelled on each curve.

3.3 Choice of the sintering and crystallisation temperatures

Some sintering tests were then performed respectively at 530, 540, 550 and 560°C (30 min). The highest shrinkage occurs at these temperatures with the matrix in the amorphous state at 530 and 540°C, but crystallising at 550 and 560°C, as observed by DSC and XRD measurements.

Some sintering processes were performed in parallel at temperatures between the T_{x1} and the maximum temperature attainable without glass melting or the expansion observed above 800°C: compacts of B3T were thermally treated for 30 min at 620 (between T_{x1} and T_{x2}), 750 (above T_{x2}) and 790°C (the upper limit before expansion, as shown in Fig. 2). These temperatures were chosen to explore if, even with a partial crystallisation of the glass matrix, the high temperature and the presence of a residual amorphous phase could enhance the viscous flow behaviour.

Density measurements were carried out, on each sintered sample. Figure 4(a) reports the Archimedean density of the sintered composite samples versus the sintering temperature. The density reached its highest value in the range between 540 and 560°C and progressively decreased as the sintering temperature increased. The highest relative density (%) calculated in respect to the pycnometric one was found at the sintering at 540°C for 30 min [Fig. 4(b)].

Some preliminary Young's Modulus measurements were performed on the composites sintered at different temperatures, and the highest value (54·8 GPa) was reached in samples sintered for 30 min at 540°C [see Fig. 4(c)].

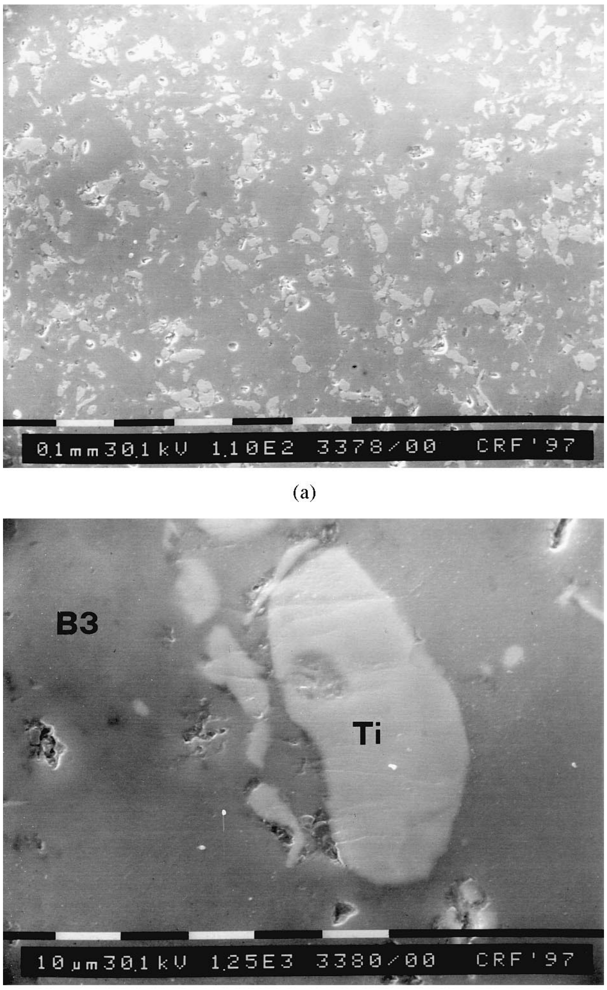

(a)

(b)

Fig. 5. General view (a) and particular (b) of the B3T glass-matrix composite sintered 30 min at 540°C.

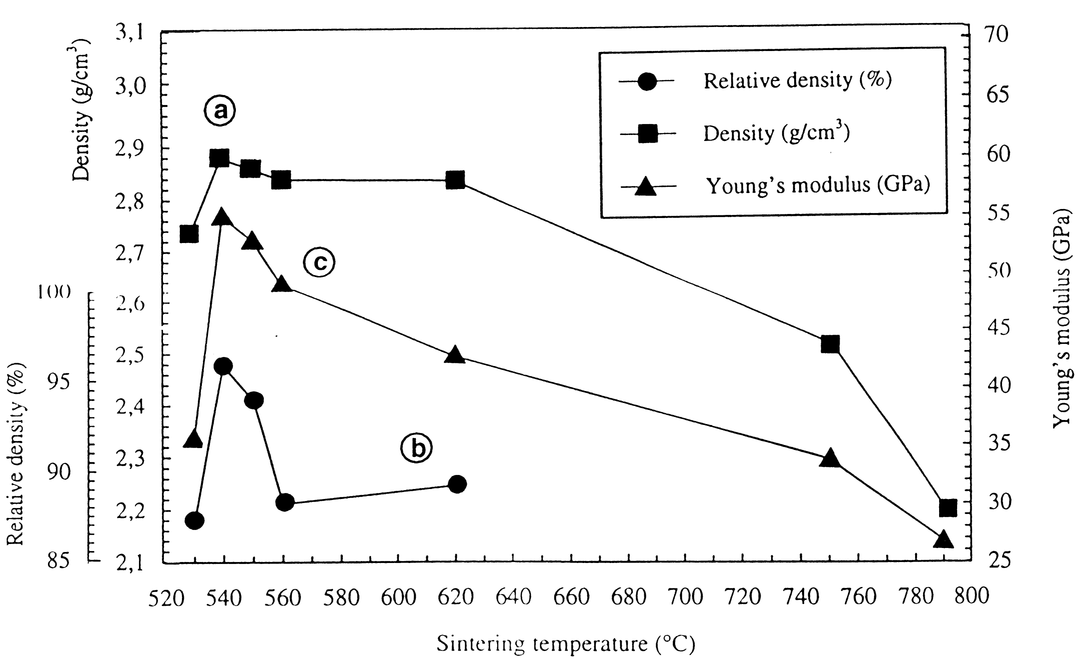

Fig. 4. (a) Archimedean densities and (b) relative densities (%) calculated in respect to the picnometric one of the sintered composites versus the sintering temperature. Young's modulus values (c) of the sintered composites, versus the sintering temperature.

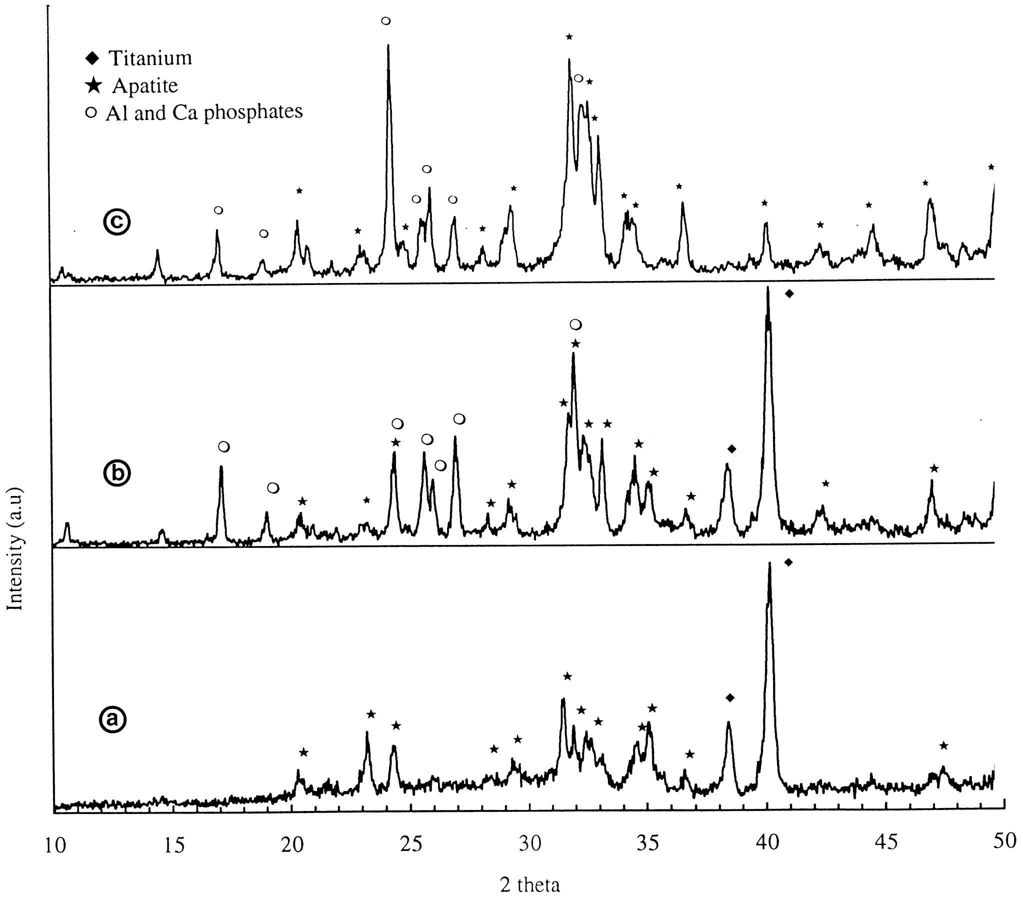

Fig. 6. XRD patterns of the glass-matrix sintered B3T composite (a), of the glass-ceramic matrix one (b) and of the pure sintered glass-ceramic (c).

XRD analyses were performed on the powdered sintered composites, in order to observe the phase formation at the different sintering temperatures. *The best compromise between high density and low crystallinity was found to be for sintering at 540°C for 30 min.*

On the basis of these results, conditions of 30 min at 540°C, in Ar flow, were chosen to prepare the sintered composites, producing a relative density of 96%. The same conditions were used to prepare pure glass sintered specimens as reference.

The morphology of the sintered glass-matrix B3T composite is shown in Fig. 5(a) (polished cross-section, not etched sample). No cracks and little porosity are visible in the glass matrix and the titanium particles are well distributed. A Ti particle in the B3T glass-matrix composite is shown in Fig. 5(b). The interface glass/metal is continuous and no cracks or bubbles between the two materials are observable (the few crystals likely to be present in the matrix are not observable with SEM on the unetched sample). For this purpose, the presence of a certain amount of TiO_2 in the glass composition is a further advantage: as reported in literature,[11,12] in order to obtain a strong bond between the glass matrix and the reinforcing metal, the adherent oxide layer normally present on the titanium surface must only partially dissolve into the softened glass. In this way a graded oxide transition layer is still present at the metal-to-glass interface, which provides a strong chemical adhesion and good stress transfer between the two materials. The presence of a certain amount of titanium oxide in the glass matrix is useful to control the oxide layer dissolution, and consequently the adherence of the glass to the titanium particles.

The B3T glass-matrix composite and the B3 glass, sintered under the optimised conditions, were crystallised for 3 h at 550°C, under Ar flow.

The EDX analysis performed on the B3 matrix (mean value of several analyses on 10–100 μm^2 area) at different stages of the composite preparation (bulk glass, composite glass matrix and composite glass-ceramic matrix) indicated no detectable compositional variation either following sintering (540°C, 30 min) or following crystallisation (550°C, 3 h)

By comparing the XRD patterns of the glass matrix composite with that of the glass–ceramic matrix composite [Fig. 6(a) and (b) respectively] it is evident that after 30 min at 540°C only apatite crystals in small amount were found [Fig. 6(a)], while after the crystallisation process (3 h at 550°C) some mixed aluminium and calcium phosphates were also formed [Fig. 6(b)]. By comparing the XRD patterns of the glass-ceramic matrix B3T composite and the pure sintered glass-ceramic

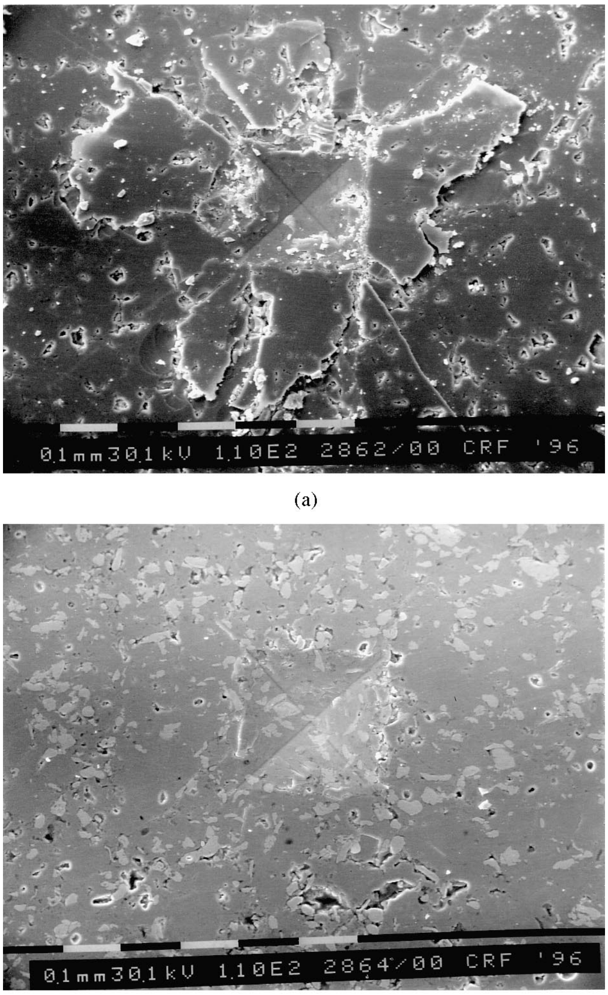

(a)

(b)

Fig. 7. Vickers indentation on the sintered B3 base glass (a) 49 N load, and on the sintered B3T glass-matrix composite (b) 98 N load.

[Fig. 6(b) and (c) respectively], it is evident that the presence of the Ti particles did not induce any crystallisation of additional phases.

3.4 Mechanical characterisation

Mechanical tests were performed both on the glass-matrix B3T composites sintered under the optimised conditions (30 min at 540°C) and on the glass-ceramic matrix composites (sintered for 30 min at 540°C and successively heated for 3 h at 550°C).

Several Vickers indentations were performed on polished sections of both the sintered pure glass and the glass-matrix composite using increasing loads, up to 98 N. The Vickers indentations at 49 N load on the sintered pure glass produced a deep crack propagation and brittle fracture of the glass surface around the indent [see Fig. 7(a)]. The composite sintered at the same time and temperature conditions shows a tougher behaviour as seen in Fig. 7(b): no cracks or brittle behaviour were observed on indenting the composite with a 98 N load.

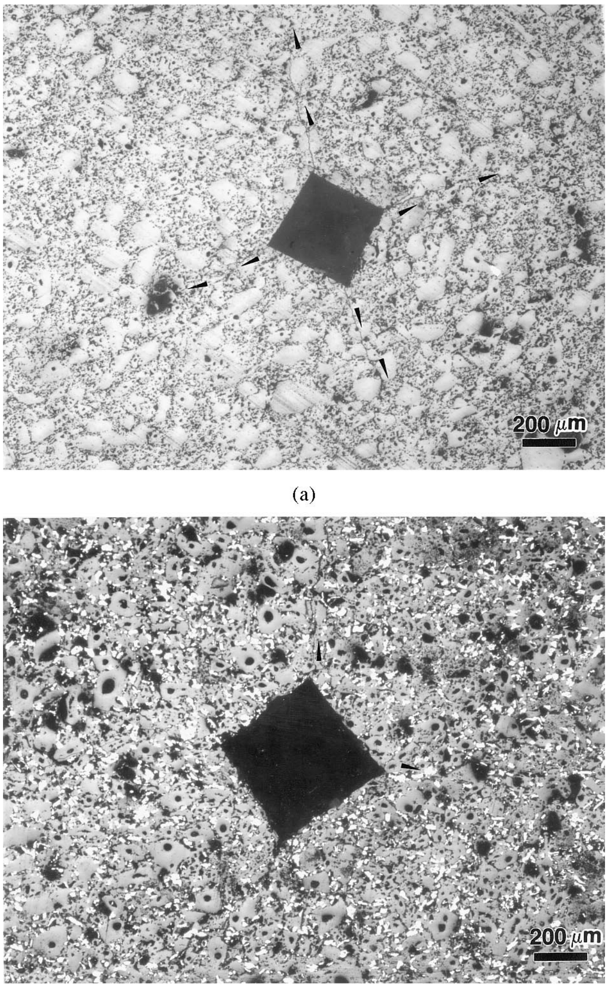

(a)

(b)

Fig. 8. Vickers indentation on the sintered B3 glass-ceramic (a) 98 N load and on the sintered B3T glass-ceramic matrix composite (b) 98 N load.

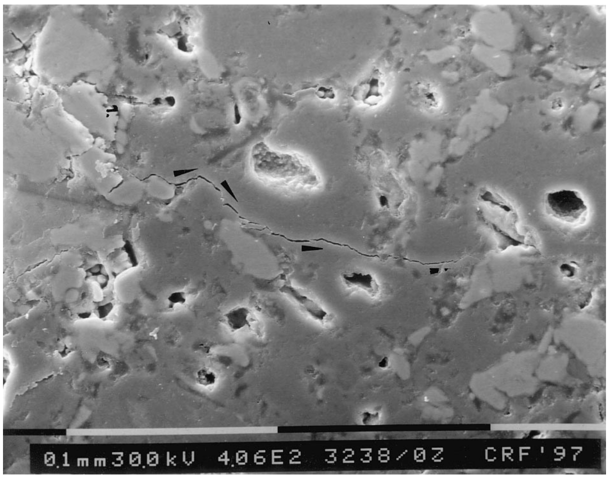

Fig. 9. Crack path induced by Vickers indentation on a B3T glass-matrix composite.

The glass-ceramic matrix B3T composite and the sintered B3 glass–ceramic were also indented with different loads up to 98 N. The composite shows a tougher behaviour in respect to the pure sintered glass-ceramic, as demonstrated in Fig. 8(a) and (b). The 98 N load indentations on the pure glass-ceramic

Table 1. Young's modulus and K_{IC} values of the sintered base glass- and glass-ceramic B3 and B3T

	Sintered B3			*Sintered B3T*	
	Glass	*Glass-ceramic*	*Glass matrix composite*	*Theoretical value (glass matrix composite)*	*Glass-ceramic matrix composite*
E (GPa ± 0·.5)	44	61	55	49–56	65
K_{IC} (MPa m$^{1/2}$ ± 0·1)	–	1·5	–	–	2·1

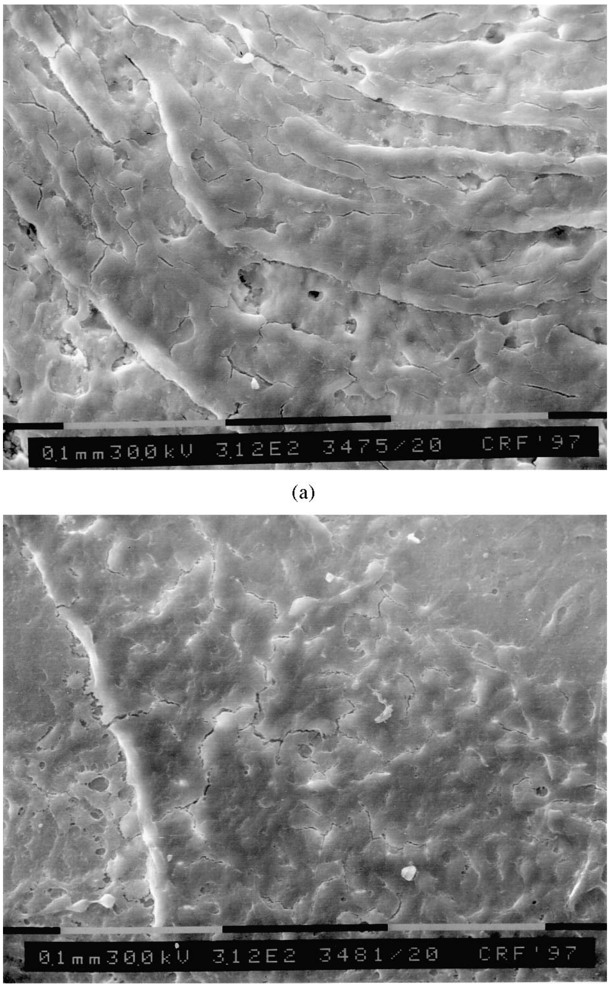

(a)

(b)

Fig. 10. Fibroblast growth on the B3T glass-ceramic composite (a) and on a reference specimen (b).

caused the propagation of 400–500 μm length cracks [Fig. 8(a)] from the indents corners, while in the case of the composite [Fig. 8(b)] the cracks induced by the same load are shorter and the indent size is larger. The toughening effect of the Ti particles embedded into the glass-ceramic B3 matrix is evident in Fig. 9 where a detail of the induced crack propagation from the Vickers tip corner (98 N) is reported: the crack path is deviated by the Ti particles.

Moreover, a tougher behaviour was shown by the glass-ceramic matrix B3T composite when compared to the glass-matrix one: by comparing Figs 7(b) and 8(b), taking into account the different magnification, it is evident that the same load (98 N) produced a larger indent on the glass-ceramic composite than that on the glass-matrix one.

The K_{IC} results were in agreement with these comparative mechanical characterisations. Even if their values are not so different from each other, they revealed a higher fracture toughness of the glass-ceramic matrix composite in respect of the pure sintered glass–ceramic (see Table 1). They are both higher than that of the bulk glass-ceramic (0·6 MPa m$^{1/2}$, as reported in Ref. 2).

Table 1 reports the Young's Modulus values of the sintered glass- and glass-ceramic B3 and B3T. Both the glass- and glass-ceramic composites have a higher Young's modulus when compared to the corresponding pure matrices, and the values are in agreement with the rule of the mixtures. These are encouraging results, since the rule of mixture is valid only if a continuous interface exists between the matrix and the particles, and if no defect (pore, cracks) is present in the bulk of the composite. Only in the case the stresses are correctly transmitted from the matrix to the reinforcing particles, making the composite tougher than the pure matrix.

3.5 Biocompatibility test

Both the biocompatibility and bioactivity of the bulk Bioverit® III glass-ceramic are well known.[2] The results of the biocompatibility test performed in this work are represented by Fig. 10(a) and Fig. 10(b), where the surface of a B3T glass-ceramic matrix composite and of a 'cell culture grade' polymeric reference specimen, after 48 h of incubation, are respectively reported. A thick 'carpet' of fibroblasts has grown on both the samples.

4 Conclusions

Bioverit® III base glass- and glass-ceramic matrix/Ti particles composites were prepared by means of a simple pressureless sintering method. The sintering process was carefully optimised by means of differential scanning calorimetry and hot stage microscopy. The sintering conditions were chosen in order to have the highest final density. The best results were reached by means of a viscous flow process, obtaining nearly full density amorphous matrix composites which were successively ceramised in order to obtain glass-ceramic matrix composites. A tougher behaviour was shown by both the glass- and glass-ceramic matrix composites when compared to the corresponding pure matrices, and by the glass-ceramic matrix composite when compared to the glass-matrix one. Fibroblasts growth on the surface of the glass-ceramic matrix composites confirms their biocompatibility.

Acknowledgements

The authors wish to thank the Fiat Research Centre (To, Italy) for SEM-EDX analysis, and the Veterinary Pathological Anatomy Institute of the University of Torino for cell cultures. This work was partially supported by the CRUI (Conferenza Permanente dei Rettori delle Universitá Italiane, 'Vigoni Program' 1995–1997).

References

1. Ducheyne, P., Marcolongo, M. and Shepers, E., Bioceramic composites. In *An Introduction to Bioceramics*, ed. L. L. Hench and J. Wilson, World Scientific, Singapore, 1993, p. 281.
2. Höland, W. and Vogel, W., Machineable and phosphate glass–ceramics. In *An Introduction to Bioceramics*, ed. L. L. Hench and J. Wilson, World Scientific, Singapore, 1993, p. 125.
3. Vogel, J., Wange, P. and Hartmann, P., Phosphate glasses and glass ceramics for medical applications. *Glastechn. Ber. Glass Sci. and Technol.*, 1997, **70**(7), 220–223.
4. Wange, P., Vogel, J., Horn, L., Höland, W. and Vogel, W., The morphology of phase formations in phosphate glass ceramics. *Silic. Ind.*, 1990, **7/8**, 231–236.
5. Ferraris, M. and Verné, E., Viscous phase sintering of particle-reinforced glass matrix composites. *J. Eur. Ceram. Soc.*, 1996, **16**, 421–427.
6. Verné, E., Ferraris, M., Manconi, M. P., Vogel, J., Jana, C. and Carl, G., Toughening of Bioverit III® glass–ceramic. In *99th ACerS Annual Meeting*, Cincinnati, Ohio, 4–7 May 1997, Abstracts Book, p. 11.
7. Verné, E., Ferraris, M., Ventrella, A., Paracchini, L., Krajewski, A. and Ravaglioli, A., Sintering and plasma spray deposition of bioactive glass-matrix composites for biomedical applications. *J. Eur. Ceram. Soc.*, 1998, **18**, 363–372.
8. Wange, P., Frigge, M., Völksch, G., Jana, C. and Götz, W., Coatings of phosphate glasses and phosphate glass–ceramic on Co–Cr- alloys. In *Advances in Science and Technology—Materials in Clinical Applications*, vol. 12, ed. P. Vincenzini, Techna Srl, 1995, p. 275.
9. Rizkalla, A. S., Jones, D. W. and Miller, R. P., Evaluation of indentation fracture toughness methods for glass biomaterials. *British Ceramic Transaction*, 1996, **95**(4), 151–156.
10. Swain, M. V. and Claussen, N., Comparison of K_{IC} values for Al_2O_3–ZrO_2 composites obtained from notched-beam and indentation strength techniques. *Am. Ceram. Soc. Comm.*, Feb. 1983, C-27.
11. Ferraris, M., Badini, C. and Couzinet, B., Interfacial equilibria in titanium particle/glass ceramic composites. *Composites*, 1994, **25**(7), 494–498.
12. Donald, I. W., Preparation, properties and chemistry of glass- and glass–ceramic-to-metal seals and coatings. *J. Mat. Sci.*, 1993, **28**, 2841.